Electric Polarization Rotation in a Hexaferrite with Long-Wavelength Magnetic Structures

T. Kimura,[1] G. Lawes,[1,*] and A. P. Ramirez[2]

[1]*Los Alamos National Laboratory, K764, Los Alamos, New Mexico 87545, USA*

[2]*Bell Laboratories, Lucent Technologies, 600 Mountain Avenue, Murray Hill, New Jersey 07974, USA*

(Received 11 November 2004; published 5 April 2005)

We report on the control of electric polarization (P) by using magnetic fields (B) in a hexaferrite having magnetic order above room temperature (RT). The material investigated is hexagonal $Ba_{0.5}Sr_{1.5}Zn_2Fe_{12}O_{22}$, which is a nonferroelectric helimagnetic insulator in the zero-field ground state. By applying B, the system undergoes successive metamagnetic transitions, and shows concomitant ferroelectric order in some of the B-induced phases with long-wavelength magnetic structures. The magnetoelectrically induced P can be rotated 360° by external B. This opens up the potential for not only RT magnetoelectric devices but also devices based on the magnetically controlled electro-optical response.

DOI: 10.1103/PhysRevLett.94.137201 PACS numbers: 75.80.+q, 64.70.Rh, 75.30.Kz

Since the theoretical prediction by Dzyaloshinskii in 1959 [1] and the first experimental observation by Astrov in 1960 [2], the study of the magnetoelectric (ME) effect, namely, the induction of electric polarization (magnetization) by applying magnetic (electric) fields, has attracted perpetual interest for more than four decades because of its potential for advanced ME devices [3–8]. However, the ME effect studied to date has been too small at low magnetic fields and/or the working temperatures are too low for practical device applications. One of the most important requirements for ME material used in practical applications is a magnetic insulator having a high magnetic ordering temperature. In this sense, ferrites, magnetic oxides containing iron as the major metallic component, are prominent candidates (I). These materials combine room temperature (RT) ferromagnetic and insulating properties and have long been used in technological applications such as magnetic recording and high-frequency devices [9,10]. Although there are several ferrites that exhibit ME effects at RT [4,8], the ME effect in these ferrites is small at low magnetic fields as in most conventional magnetoelectrics. Recent discoveries of a large ME effect in $TbMnO_3$ [11] and $DyMnO_3$ [12] imply the possibility of a strong interplay between magnetization and electric polarization in insulating systems with long-wavelength magnetic structures (e.g., sinusoidal, spiral) (II). Combining these two strategies (I and II), we demonstrate remarkable ME response in a hexaferrite, $Ba_{0.5}Sr_{1.5}Zn_2Fe_{12}O_{22}$, having helimagnetic ground-state and magnetic order above RT.

Figure 1(a) shows the crystal structure of $Ba_{2-x}Sr_xZn_2Fe_{12}O_{22}$ (magnetoplumbite-related Y-type hexaferrite) [9,13]. The fundamental structure belongs to the space group $R\bar{3}m$ ($Z = 3$) which does not allow for a spontaneous electric polarization (P_s). To understand the ground-state magnetic structure of this system [14–17], it is convenient to consider that $Ba_{2-x}Sr_xZn_2Fe_{12}O_{22}$ is composed of alternating stacking of the L and S blocks along the c axis [Fig. 1(a)]. Within these blocks, the magnetic moments on Fe sites lying in the ab plane are collinear and form ferrimagnetic structures. (The magnetic anisotropy in the ab plane is negligible.) The effective moments of the L and S blocks are $\mu_L = (3 + 2\gamma)\mu_{Fe}$ and $\mu_S = (2\gamma - 1)\mu_{Fe}$, respectively. [Here, μ_{Fe} is the moment per Fe ion and γ is a fraction of Zn ions in (Zn, Fe) sites in the L block.] The boundary of these spin blocks is located between the Fe(4) and Fe(5) sites [see Fig. 1(a)]. The superexchange interaction across the boundary of these blocks, Fe(4)-O(2)-Fe(5), can be tuned by replacing Ba with Sr due to the size difference between Ba and Sr ions. The Sr-free ($x = 0$) crystal shows collinear ferrimagnetic

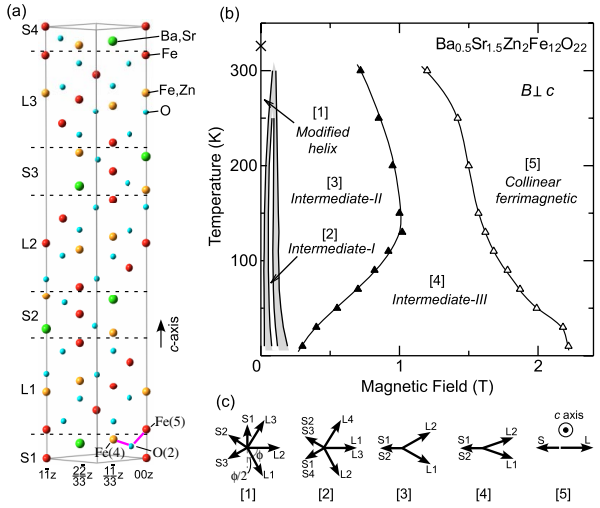

FIG. 1 (color online). (a) Schematic crystal structure of $Ba_{2-x}Sr_xZn_2Fe_{12}O_{22}$. (b) Magnetic phase diagram of the crystal used in this study, which was determined by measurements of M in the B-increasing runs with $B \perp c$. A cross denotes T_N. Grey area corresponds to phase boundaries. (c) Proposed models [16,17] for the evolution of magnetic structures by applying $B \perp c$. The long and short arrows indicate μ_L and μ_S, respectively. The numbers below each model corresponds to those in (b).

order (Néel temperature, $T_N = 392$ K) with a parallel arrangement of the Fe(4) and Fe(5) moments, whereas the Sr-rich ($x > 1.6$) crystals show antiferromagnetic order with an antiparallel arrangement. In the intermediate x region ($1.0 < x < 1.6$), the focus of this Letter, the system develops a noncollinear helical spin structure characterized by the angle between the effective moments of neighboring L and S blocks ($180° - \phi/2$) [Fig. 1(c)]. For example, ϕ in an $x = 1.5$ crystal is 83.4° at 8 K, and increases with increasing temperature (T), to become 180° by 319 K [17].

We have grown single crystals of $Ba_{0.5}Sr_{1.5}Zn_2Fe_{12}O_{22}$ from Na_2O-Fe_2O_3 flux, following Ref. [18]. For the measurements of the dielectric constant (ε) at 100 kHz and the ME current (J_{ME}), the grown crystals were formed into rectangular thin plates with the widest faces including the c axis, and gold electrodes were sputtered onto the widest faces. J_{ME} was measured with an electrometer while sweeping magnetic fields (B) at a rate of 0.02 T/s. The electric polarization (P) was obtained by integrating J_{ME} as a function of time.

The helical spin structure in $Ba_{0.5}Sr_{1.5}Zn_2Fe_{12}O_{22}$ is modulated by the application of B perpendicular to the c axis [16,17]. We display in Fig. 1(b) the magnetic phase diagram for $Ba_{0.5}Sr_{1.5}Zn_2Fe_{12}O_{22}$ ($T_N = 326$ K). The B-T phase diagram bears a close resemblance to that presented in Ref. [17]. Figure 1(c) shows the proposed models [16,17] for the evolution of the magnetic structures by the application of B. In the helimagnetic phase at weak B, the modulation wave vector for the helix $(0, 0, 3\delta)$ is incommensurate ($0 < \delta < 1/2$). In contrast, those in the intermediate-I, intermediate-II, and intermediate-III phases are commensurate; the δ values for these intermediate phases are $1/4$, $1/2$, and $1/2$, respectively [16].

Previous studies for certain rare-earth manganites [5,11,12,19,20] suggest that materials having long-wavelength magnetic structures often exhibit a strong interplay between magnetic ordering and ferroelectricity, which makes $Ba_{0.5}Sr_{1.5}Zn_2Fe_{12}O_{22}$ a good magnetic ferroelectric candidate. Figure 2 displays the B dependence of the magnetization (M), the relative change in ε (i.e., magnetocapacitance; $\Delta\varepsilon(B)/\varepsilon(0) = [\Delta\varepsilon(B) - \varepsilon(0)]/\varepsilon(0)$), J_{ME}, and P for a crystal of $Ba_{0.5}Sr_{1.5}Zn_2Fe_{12}O_{22}$ at 10 K. The experimental configurations used for these measurements are illustrated in Fig. 2(h), and B was applied perpendicular to the c axis in all cases. For measurements of $\Delta\varepsilon(B)/\varepsilon(0)$ and J_{ME}, the electric field (E) and the current were perpendicular to both the c axis and the direction of B. As illustrated in Figs. 2(a) and 2(e), M increases in a stepwise fashion. These features are attributed to the successive evolution in magnetic structures shown in Fig. 1. The first ($0 < B < \sim 0.025$ T), the second ($\sim 0.07 < B < \sim 0.11$ T), and the third ($\sim 0.18 < B < \sim 0.3$ T) terraces in M, correspond to the slightly modified helimagnetic, intermediate-I, and intermediate-II phases, respectively. The intermediate-III phase corresponds to the

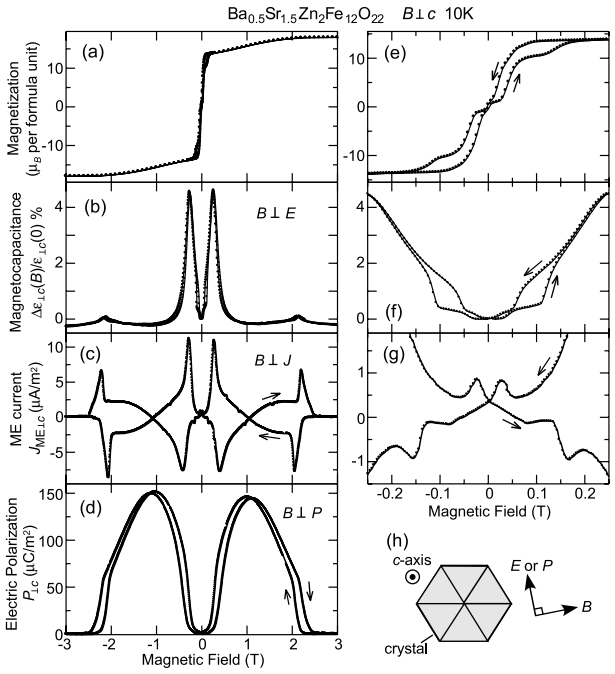

FIG. 2. (a) M, (b) $\Delta\varepsilon(B)/\varepsilon(0)$, (c) J_{ME}, and (d) P of $Ba_{0.5}Sr_{1.5}Zn_2Fe_{12}O_{22}$ as a function of B at 10 K. (e),(g) Expanded views of a potion of (a)–(c), respectively. (h) Schematic experimental configurations. For the measurement of J_{ME}, $E = 220$ kV/m was continuously applied during the measurement to keep the crystal as single ferroelectric domains in the intermediate phases.

magnetic field range with a rather large slope in M ($\sim 0.3 < B < \sim 2.2$ T). Upon further increasing B, M finally saturates at ~ 2.2 T where the collinear ferrimagnetic phase appears. As seen in Figs. 2(b) and 2(c), $\Delta\varepsilon(B)/\varepsilon(0)$ and J_{ME} show remarkable peak structures centered at the magnetic phase boundaries between the intermediate-II and intermediate-III phases, and between the intermediate-III and collinear ferrimagnetic phases. In the low B region, $\Delta\varepsilon(B)/\varepsilon(0)$ exhibits hysteresis and stepwise structures similar to those observed in M [Fig. 2(f)] and some anomalies are observed in J_{ME} [Fig. 2(g)].

The B dependence of P, obtained from integrating J_{ME}, reveals the origin of the anomalies in $\Delta\varepsilon(B)/\varepsilon(0)$ and J_{ME}. As displayed in Fig. 2(d), there is no P_s at $B = 0$. By applying B, P is gradually developed, and shows a rapid increase at the phase boundary between the intermediate-II and intermediate-III phases. With increasing B, P reaches a maximum ($\sim 150\ \mu$C/m^2) at ~ 1 T, and finally vanishes close to the phase boundary between the intermediate-III and collinear ferrimagnetic phases. The sign of this induced P is independent of that of B [Fig. 2(d)], but dependent on that of the applied E.

To further examine the effect of B on ε and P, we explored the T dependence of these quantities. The intermediate-III phase is indicated by the B region between the open triangles in Fig. 3(a) for various temperatures. We

see that the peaks in $\Delta\varepsilon(B)/\varepsilon(0)$ trace out the boundaries of the intermediate-III phase both at low and high B. Although the P-B data in Fig. 2(d) were taken in applied electric fields, even at $E = 0$ we also see at the intermediate-III phase that the system possesses the same magnitude of P_s after a proper poling procedure [Fig. 3(c)]. In addition, the sign of P can be reversed by poling E. These results clearly demonstrate that the application of a moderate B induces a phase in which polarity can be switched by poling E, namely, a ferroelectric phase. Figure 3 clearly shows the intimate connection between magnetic order in the intermediate-III phase and ferroelectricity in $Ba_{0.5}Sr_{1.5}Zn_2Fe_{12}O_{22}$. The origin of breaking space inversion symmetry in the ferrite is likely caused by a magnetoelastically induced lattice modulation similar to that observed in magnetic ferroelectric rare-earth manganites with long-wavelength magnetic structures [11,12].

It is worth noting that the intermediate-III phase persists up to RT [see Fig. 1(b)]. This indicates that $Ba_{0.5}Sr_{1.5}Zn_2Fe_{12}O_{22}$ displays B-induced ferroelectric order at temperatures close to RT, though the resistivity above $\sim$130 K of the crystal studied here becomes too low to permit poling by high E. In addition, the transition occurs at rather low B below 1 T. Thus, the hexaferrite

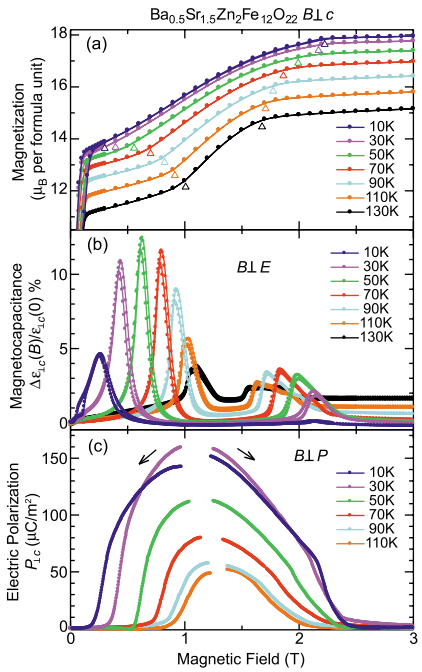

FIG. 3 (color online). (a) M, (b) $\Delta\varepsilon(B)/\varepsilon(0)$, and (c) P of $Ba_{0.5}Sr_{1.5}Zn_2Fe_{12}O_{22}$ as a function of B at various Ts. The experimental configurations are the same as those shown in Fig. 2(h). To pole the crystal, $E = 220$ kV/m was applied at $B = 0$, and then B was set to drive the system to a range of intermediate-III phases. After these procedures, the poling E was removed, and J_{ME} was measured during the B decreasing [for lower-field data ($B < \sim 1.2$ T)] or increasing [for higher-field data ($B > \sim 1.2$ T)] runs.

having long-wavelength magnetic structures exhibits remarkable ME responses at low B and above liquid nitrogen temperature, which opens substantial possibilities for applications of ME systems.

$Ba_{0.5}Sr_{1.5}Zn_2Fe_{12}O_{22}$ displays an additional type of ME coupling, namely, magnetically rotatable ferroelectric polarization. This type of control over the polarization direction using B provides the possibility of novel devices based on a magnetically controlled electro-optical response, suggesting an analogy with liquid crystals where the polarization direction is controlled by E. The symmetry-based analysis of the ME effect [21] allows the continuous rotation of P by changing the direction of B. There have been several reports of polarization rotation in magnetoelectrics [22,23]. However, the effects studied to date are rather small and/or the working temperature is too low for practical applications. Our results show that a large P_s in $Ba_{0.5}Sr_{1.5}Zn_2Fe_{12}O_{22}$ emerges when B is applied perpendicular to the c axis, and the direction of P_s is perpendicular to both B and the c axis [see Fig. 2(h)]. Therefore, we expect that the B-induced polarization can be rotated continuously in the ab plane by changing the direction of B.

To test this prediction, we performed the following experiment. To begin, $E = 220$ kV/m was applied perpendicular to the c axis at $B = 0$. Then $B = 1.1$ T was applied perpendicular to both E and the c axis [left inset of Fig. 4(b)]. These steps poled the B-induced ferroelectric phase. After poling, E was turned off. This initial orientation of B and P_s corresponds to $\theta = 0°$. Next, B was rotated through θ in the ab plane, and J_{ME} was measured [right inset of Fig. 4(b)]. Figure 4(a) displays the B-dependence of P at 20 K for various values of θ. The data at $\theta = 0°$ show the appearance of P_s induced by a moderate B, as discussed above. As θ is increased towards 90°, the component of P along the direction between the electrodes gradually decreases in the ferroelectric phase and becomes zero at 90° where the direction of B is parallel to the measured J_{ME}. Upon further increasing θ, P becomes negative, and is totally reversed at $\theta = 180°$. Figure 4(b) shows the θ dependence of P at $B = 1$ T, which can be fit to the function $\cos\theta$ [solid curve in Fig. 4(b)]. These results show that as we rotate B in the θ plane the direction of P also rotates to remain perpendicular to B.

In terms of a symmetry-based analysis of the ME coefficient [21], the magnetically rotatable polarization observed at the intermediate-III phase of $Ba_{0.5}Sr_{1.5}Zn_2Fe_{12}O_{22}$ should be dominated by the linear ME effect. Although the complex B dependence of P shown in Fig. 3(c) reminds us of the existence of a ME effect of higher order than bilinear, it is ascribed to the existence of B-induced phase transitions which change the magnetic symmetries. To determine the character of the ME effect in such systems, we may need to analyze the data in each phase separately. The measurements for the

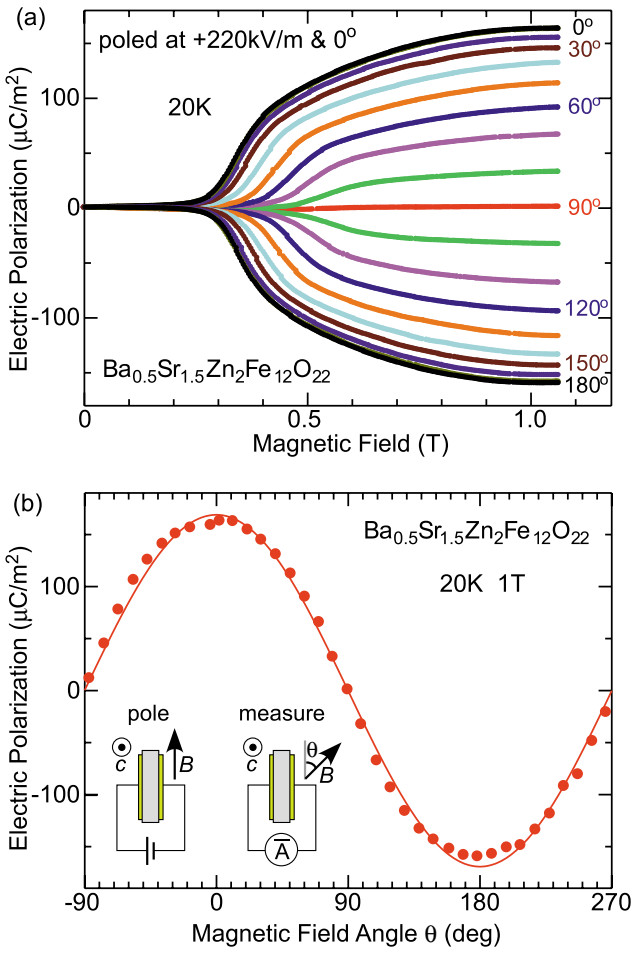

FIG. 4 (color online). (a) P loaded with B at angle θ in the range 0°–180° (every 10°) from the poling direction. (b) Angle dependence of P at $B = 1$ T. Schematic pictures of experimental configurations are shown in the inset.

θ-dependence data in Fig. 4 are appropriate to determine the order of the ME effect at the intermediate-III phase, because the magnetic phase never changes during the measurements. Supposing the magnetic symmetry of intermediate-III phase is $\bar{3}'m$ where the linear ME coefficients [α_{12} and $\alpha_{21} = (-\alpha_{12})$] are allowed [21], the cosθ dependence of P shown in Fig. 4(b) can be explained. Thus, the direction of P_s can be turned full circle by using B in $Ba_{0.5}Sr_{1.5}Zn_2Fe_{12}O_{22}$, a phenomenon which might also be useful for magnetic control of the electro-optical response.

In summary, the strong interplay of electric polarization and magnetization observed in $Ba_{0.5}Sr_{1.5}Zn_2Fe_{12}O_{22}$ opens up a new direction for applications of hexaferrites having structures related to magnetoplumbite (e.g., $BaFe_{12}O_{19}$) [9], which have long been used for permanent magnets and are of interest for microwave devices [10]. The results presented here also provide a novel aspect for the study of magnetic insulators with long-wavelength magnetic structures, namely, the study of their magnetoelectric response.

We thank S. M. Shapiro, G. Xu, and A. V. Balatsky for discussions, and J. L. Sarrao and E. D. Bauer for help with experiments. This work was supported by the U.S. DOE.

*Present address: Department of Physics and Astronomy, Wayne State University, Detroit, MI 48201.

[1] I. E. Dzyaloshinskii, Sov. Phys. JETP **10**, 628 (1960).
[2] D. N. Astrov, Sov. Phys. JETP **11**, 708 (1960).
[3] T. H. O'Dell, *The Electrodynamics of Magneto-Electric Media* (North-Holland, Amsterdam, 1970).
[4] G. T. Rado, Phys. Rev. Lett. **13**, 335 (1964).
[5] H. Wiegelman *et al.*, Physica (Amsterdam) **204B**, 292 (1995).
[6] H. Nakamura and K. Kohn, Ferroelectrics **204**, 107 (1997).
[7] I. Kornev *et al.*, Phys. Rev. B **62**, 12 247 (2000).
[8] J. Wang *et al.*, Science **299**, 1719 (2003).
[9] J. Smit and H. P. J. Wijn, *Ferrites* (Phillips Technical Library, Eindhoven, The Netherlands, 1959).
[10] M. Sugimoto, J. Am. Ceram. Soc. **82**, 269 (1999).
[11] T. Kimura *et al.*, Nature (London) **426**, 55 (2003).
[12] T. Goto *et al.*, Phys. Rev. Lett. **92**, 257201 (2004).
[13] P. B. Braun, Philips Res. Rep. **12**, 491 (1957).
[14] U. Enz, J. Appl. Phys. **32**, 22S (1961).
[15] V. A. Sizov *et al.*, Sov. Phys. JETP **26**, 736 (1968).
[16] N. Momozawa *et al.*, J. Phys. Soc. Jpn. **54**, 771 (1985); **54**, 3895 (1985).
[17] N. Momozawa and Y. Yamaguchi, J. Phys. Soc. Jpn. **62**, 1292 (1993).
[18] N. Momozawa *et al.*, J. Cryst. Growth **83**, 403 (1987).
[19] N. Hur *et al.*, Nature (London) **429**, 392 (2004).
[20] S. Kobayashi *et al.*, J. Phys. Soc. Jpn. **73**, 1031 (2004).
[21] R. R. Birss, *Symmetry and Magnetism* (North-Holland, Amsterdam, 1966).
[22] M. Luján *et al.*, Ferroelectrics **162**, 69 (1994).
[23] Y. Koyata and K. Kohn, Ferroelectrics **204**, 115 (1997).